Study of the Isomers of Isoelectronic C_4, $(C_3B)^-$, and $(C_3N)^+$: Rearrangements through Cyclic Isomers

Tianfang Wang,[†] Mark A. Buntine,[‡] and John H. Bowie*,[†]

Department of Chemistry, The University of Adelaide, South Australia, 5005, and Department of Chemistry, Curtin University of Technology, GPO Box U1987, Perth, Western Australia

Received: August 3, 2009; Revised Manuscript Received: September 23, 2009

Optimized structures of the isoelectronic cumulenes $(CCCB)^-$, CCCC, and $(CCCN)^+$ and of their isomers formed by rearrangement have been calculated at the B3LYP/6-311+ G(3df) level of theory with relative energies and electronic states determined at the CCSD(T)/aug-cc-pVTZ level of theory. The ground states of CCCC and $(CCCN)^+$ are triplets, whereas the ground state of $(CCCB)^-$ is a quasi-linear singlet structure that is only 0.6 kcal mol^{-1} more negative in energy than the linear triplet. When energized, both triplet and singlet CCCC cyclize to planar rhomboids, of which the singlet is the lowest-energy configuration. Ring-opening of rhomboid C_4 reforms CCCC with the carbons partially randomized. Similar rearrangements occur for $(CCCB)^-$ and $(CCCN)^+$, but the reactions are different in the detail. In the case of $(CCCN)^+$, rearrangement of atoms is supported both experimentally and theoretically. Because $(CCCB)^-$ and $(CCCN)^+$ are not symmetrical, two fully cyclized forms are possible; the one more resembling a rhomboid structure is called a "kite" structure, and the other is called a "fan" structure. The rearrangement of $(CCCB)^-$ is more favored via the triplet with equilibrating kite and fan structures being formed, whereas the singlet $(CCCN)^+$ ring closes to give the singlet kite structure, which may ring open to give a mixture of $(CCCN)^+$ and $(CCNC)^+$. Intersystem crossing may occur for the triplet and singlet forms of CCCC and $(CCCB)^-$ but not for $(CCCN)^+$.

1. Introduction

The chemistry of cumulenes (carbon clusters) is of importance in combustion processes, materials science, and interstellar chemistry.[1] We have previously studied the reactivity of energized CCCC,[2] CCCN,[3] CCCO,[4] and CCCS[4] by experiment and theory, together with CCCB,[5] CCCSi,[6] CCCP,[6] and CCCAl[5] by theory alone. Of these, linear CCCC,[7] CCCN,[8] CCCO,[9–11] and CCCS[9–11] have been detected in interstellar molecular clouds, as has cyclic C_3Si.[12,13] With the exception of energized CCCO (which decomposes to CC and CO) and CCCS (which fragments to give CCC and S), other systems cyclize to give rhomboid structures. Linear CCCC is the only one of these systems that can cyclize to give a true rhombus; other structures can cyclize to give kite and fan structures; often, the kite and fan structures are interconvertible.[3,5,6] The cyclic structures drawn below show bond connectivities but not bond multiplicities. It is not a simple matter to represent such multiply bonded cyclic structures using the valence bond theory, even invoking contributing structures of a resonance hybrid.

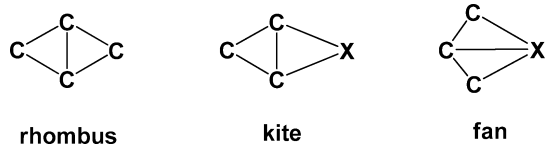

rhombus kite fan

The planar cyclic structures are both unusual and interesting. They are relatively stable species with respect to the linear CCCX isomers. As early as the 1970s, it was proposed that neutral C_4 should have a cyclic ground state, and that the cyclic form might be present in interstellar regions.[14] Linear CCCC has a $^3\Sigma_g$ ground state that is 2.8 kcal mol^{-1} less stable than rhombic C_4 (^1A_g) at the CCSD(T)/aug-cc-pVDZ//B3LYP/6-31G(d) level of theory;[2] other theoretical studies indicate that the two structures are virtually isoenergetic.[15–17] Scrambling of the atoms of CCCX following equilibration with 'rhomboid'-type isomers was first noted experimentally (using ^{13}C labeling) for CCCC,[2] then for CCCCC,[18] and finally for CCCN.[3] Analogous equilibria are predicted theoretically for CCCB,[5] CCCSi,[6] and CCCP[6] but not for CCCAl. (Energized CCCAl should form equilibrating kite and fan forms, but ring-opening of these cyclic isomers will reform CCCAl rather that giving CCAlC.[5])

Following our earlier work on CCCX systems, we seek to explore the structures and chemistry of $(CCCB)^-$ and $(CCCN)^+$, two systems that are isoelectronic with CCCC. This work is important for two reasons: (i) To obtain data concerning relative trends in structure, bonding, and reactivity of the isoelectronic systems. Detailed information on the relevant molecular orbitals of the isoelectronic species as well as singlet−triplet (S/T) energy gaps suggest molecular reactivity and provide direct insight into the subtle balance of orbital energies and correlation effects. (ii) Both $(CCCB)^-$ and $(CCCN)^+$ are potential interstellar molecules. A particular example of the importance of investigations of isoelectronic cumulene systems is the theoretical study of C_5N_2 and C_6N_2 and isoelectronic C_nO, C_nH_2, C_nN^-, and $C_nO_2^{2+}$, where it was shown that odd-numbered carbon clusters had triplet ground states and cumulenic structures, whereas even-numbered carbon clusters had singlet ground states and polyacetylenic structures.[19]

Cumulene CCCC and its rhombus have been previously studied both experimentally and theoretically,[2] and CCCC has recently been confirmed as an interstellar molecule.[7] This study

* Corresponding author.
[†] The University of Adelaide.
[‡] Curtin University of Technology.

10.1021/jp907484z CCC: $40.75 © 2009 American Chemical Society
Published on Web 10/09/2009

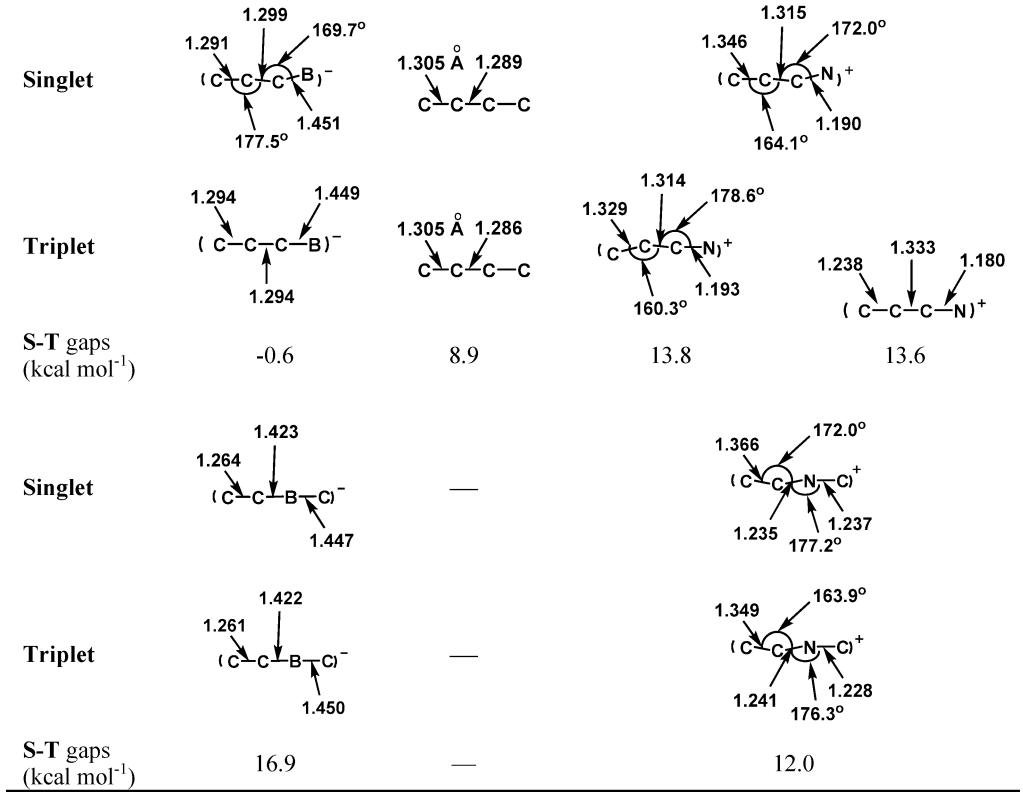

Figure 1. Geometries and singlet−triplet energy gaps of the isoelectronic linear structures of $(C_3B)^-$, C_4, and $(C_3N)^+$. CCSD(T)/aug-cc-pVTZ//B3LYP/6-311+G(3df) level of theory. Positive values indicate the triplet being lower in energy.

of CCCC is theoretical and confirms experimental findings but uses a higher level of theory than that used previously. The present study of $(CCCB)^-$ is also purely theoretical because we have been unable to devise a synthesis of this anion in the mass spectrometer by an unequivocal route.[2] Nothing has been reported of $(CCCB^-)$, although BC^-[20] and CCB^-[21,22] are known.

The final system, $(CCCN)^+$, has been studied experimentally[3] (using ^{13}C labeled analogues) and here using theory. The cation $(CCCN)^+$ may be formed by electron-impact ionization of cyanoacetylene[23] or C_4N_2[24] or by synchronous loss of two electrons from $(CCCN)^-$.[3] Linear $(CCCN)^+$ and cyclic C_3N^+ isomers have been investigated by theory,[23,25,26] and the gas-phase ion molecule chemistry of $(CCCN)^+$ has been studied.[27,28]

The present study seeks to answer the following questions: (i) are there trends in the structures of linear, kite, and fan isomers of the three isoelectronic systems, (ii) what are the ground states and singlet−triplet energy gaps of isomers in the three systems, (iii) what are the mechanisms and energetics of any cyclization/rearrangement processes, and (iv) having formed the cyclic isomers, can these ring open to effect atom scrambling within the cumulene ?

2. Computational Section

Geometry optimizations were carried out with the Gaussian 03 suite of programs[29] using the Becke RB3LYP (singlets) or UB3LYP (triplets) method with the split-valence 6-311+G(3df) basis set.[30,31] Stationary points were determined by calculation of the frequencies using analytical gradient procedures according to the principle of either minima (no imaginary frequencies) or transition states (one imaginary frequency). The minima connected by a given transition structure were confirmed by intrinsic reaction coordinate (IRC) calculations. Single-point energies for the B3LYP/6-311+G(3df) geometries were determined using the CCSD(T) method together with the Dunning aug-cc-pVTZ basis set,[32–34] including zero-point energy correction (unscaled).

We obtained approximate minimum energy crossing points by carrying out geometry optimizations at a series of points along an appropriate coordinate that, in principle, connects the minimum on one electronic surface with the minimum on the other electronic surface using the CASSCF method. The CASSCF/6-311+G(3df) spin−orbit coupling constants (SOC) were computed at the crossing points using a one-electron approximation.[35–38] The details of active spaces chosen for the CCCX (X represents B, C, or N) involve the σ(CX), the two σ(CC), the π, and the corresponding antibonding orbitals. For kite structures $(C_3N)^+$, the $\sigma(C_3N)$, $\sigma(C_1C_2)$, $\sigma(C_1C_3)$ (see Figure 3 for a definition of the number-labeled structure), and π orbitals and the corresponding antibonding orbitals have been taken into consideration.

All calculations were performed using the South Australian Partnership for Advanced Computing (SAPAC) facility

3. Results and Discussion

3.1. Structures of Linear Isomers. The structures of CCCC have been reported at the CCSD(T)/aug-cc-pVDZ//B3LYP/6-31G(d) level of theory.[2] This has been upgraded to CCSD(T)/aug-cc-pVTZ//B3LYP/6-311+G(3df) in this article to allow direct comparison with the calculated structures of $(CCCB)^-$ and $(CCCN)^+$. Data provided using the two different levels of theory for CCCC are very similar. The geometries and relative energies of the singlet and triplet forms of the five isoelectronic linear structures, that is, $(CCCB)^-$, $(CCBC)^-$, CCCC, $(CCCN)^+$, and $(CCNC)^+$, are shown in Figure 1 with full details recorded in Table 1 of the Supporting Information. The electronic configurations of the singlet and triplet structures together with

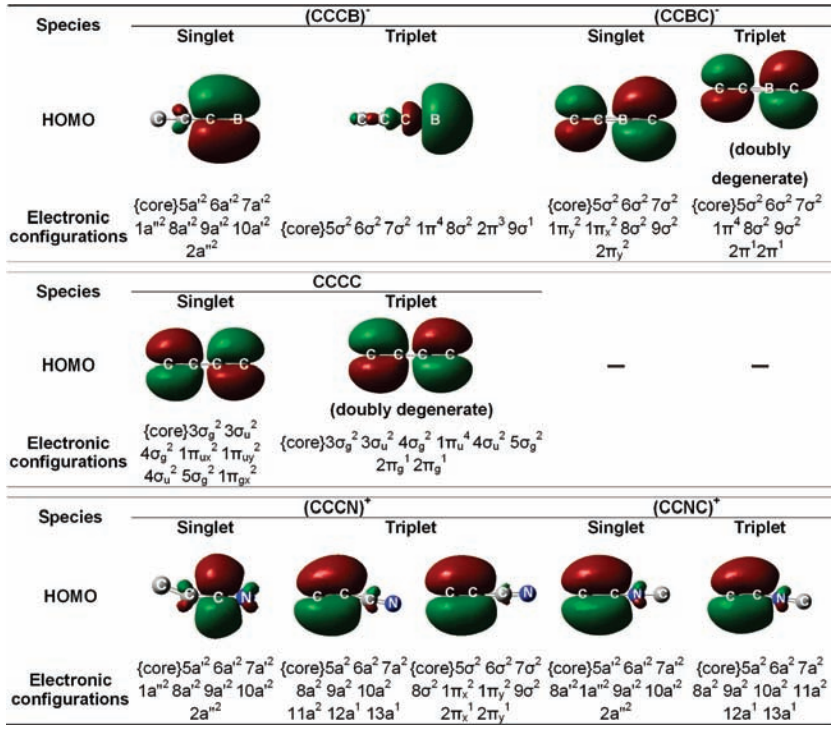

Figure 2. Electronic configurations and 3D HOMOs of the singlet and triplet isoelectronic linear structures. B3LYP/6-311+G(3df) level of theory.

representations of their highest occupied molecular orbitals (HOMOs) are recorded in Figure 2.

The triplet ($^3\Sigma_g$) form of CCCC with $D_{\infty h}$ symmetry is the ground state by 8.9 kcal mol^{-1}, with the HOMOs being doubly degenerate. The structure of the corresponding singlet ($^1\Sigma_g$) is very similar to that of the triplet (Figures 1 and 2) with all bonds showing significant double-bond character (C═C, 1.34 Å[39]).

The structures of the linear $(C_3B)^-$ isomers are more complex than the CCCC structures. The singlet ($^1A'$) form of $(CCCB)^-$ with C_s symmetry is the ground state, but this structure is only 0.6 kcal mol^{-1} lower in energy than the $^3\Sigma^-$ triplet structure, and it is possible that these two structures may interconvert by spin−orbital coupling. The $^1\Sigma^-$ linear $(CCCB)^-$ structure with $C_{\infty h}$ symmetry is unstable at the level of theory used in this study with an imaginary frequency of 137i cm^{-1} and is ∼29.0 kcal mol^{-1} above the ground state. It is likely that these two structures may convert to each other via rovibrational coupling between the motions of electrons and nuclear vibrations (the Renner−Teller effect).[40] The triplet $^3\Sigma^-$ state of linear $(CCCB)^-$ has a different electronic configuration than that of triplet $^3\Sigma_g$ CCCC. The valence AO−MO correlation diagram (at the B3LYP/6-311+G(3df) level of theory) of the linear structure $(CCCB)^-$ is shown in Figure 3. (For the AO−MO correlation diagram of CCCC, see Figure 1 of the Supporting Information.) The energy gap between the 2p and 2s orbitals of boron is 5.6 eV, whereas the corresponding energy gap for carbon is 8.8 eV. As a consequence, the 2s orbital of boron has more perturbation of the p_z orbital, which in turn leads to a significant contribution from the 2s atomic orbital to the 9σ molecular orbital. This results in the 9σ molecular orbital being above 2π for triplet $(CCCB)^-$ (Figure 2). The bond lengths of the bent singlet and linear triplet forms of $(CCCB)^-$ are similar (Figure 1), with CC and CB bonds both showing significant double-bond character. (The bond length of a CB single bond is reported to be 1.56 Å.[41])

In contrast with $(CCCB)^-$, the triplet $^3\Sigma^-$ form of $(CCBC)^-$ ($C_{\infty v}$ symmetry) is the ground state by 16.9 kcal mol^{-1}. This

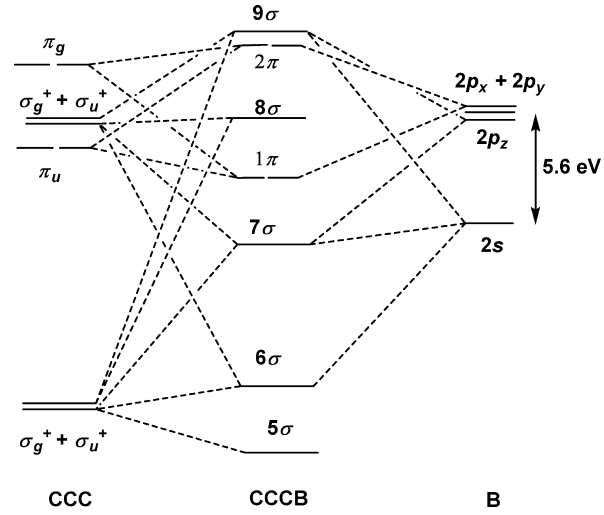

Figure 3. Valence AO−MO correlation diagram of linear $(CCCB)^-$.

can be attributed to the doubly degenerate nature of its π orbitals shown in Figure 2. Both singlet and triplet states have similar geometries: they are both linear with all bonds having significant double-bond character, as is the case with CCCC. This may be due to analogous electronic configurations of these two states. The valence AO−MO correlation diagram for $(CCBC)^-$ is shown in Figure 4. When the boron atom is located between two carbon atoms, the perturbation among the 2p orbitals (the 2p orbital energies of boron and carbon atoms are close; −5.2 and −7.3 eV respectively) becomes dominant, which results in four high-energy linear CBC π orbitals. (See Figure 1 of the Supporting Information for details.) By correlating with the $2p_x$ and $2p_y$ orbitals of another carbon atom, they form doubly degenerated 2π HOMOs, which are located at a higher energy level than the 9σ orbital, resulting in π orbital splitting (π_y and π_x) for the singlet structure. The HOMO electrons of the singlet

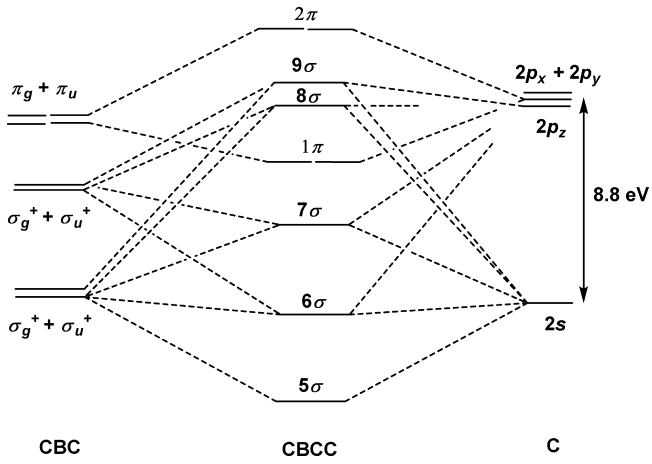

Figure 4. Valence AO−MO correlation diagram of linear $(CCBC)^-$.

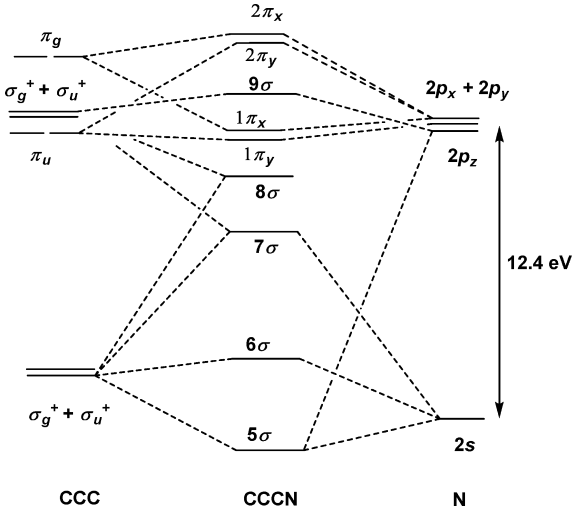

Figure 5. Valence AO−MO correlation diagram of linear $(CCCN)^+$.

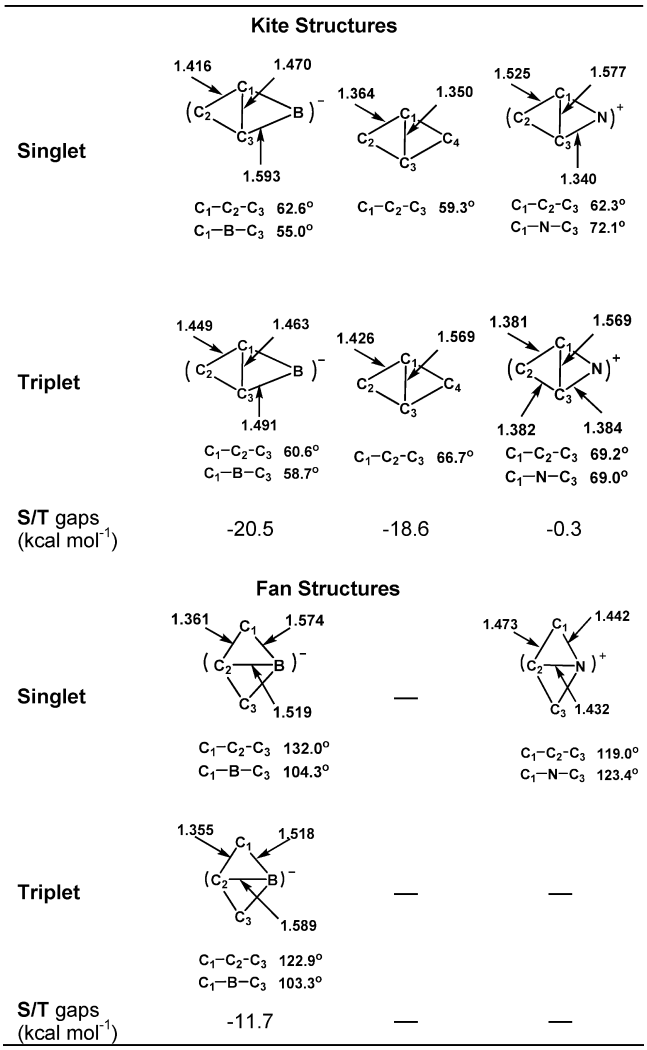

Figure 6. Geometries and singlet−triplet energy gaps of the isoelectronic cyclic structures of $(C_3B)^-$, C_4, and $(C_3N)^+$. CCSD(T)/aug-cc-pVTZ//B3LYP/6-311+G(3df) level of theory. Positive values indicate the triplet being lower in energy.

structure are mainly distributed between B and C_1 (for numbering system, see Table 1 of the Supporting Information): this should be compared with the near-equal distribution of electrons among the four atoms of the triplet. As a result, the C_2C_3 bond length becomes shorter (by 0.003 Å), whereas the BC_1 bond length is increased by some 0.003 Å for the triplet.

Linear $(CCCN)^+$ and $(CCNC)^+$ are the most complex of the linear isomers considered in this study. Calculations of the systems have been previously reported.[23,25,26] At the level of theory used in this study, the ground state of $(CCCN)^+$ is the triplet quasi-linear structure with C_1 symmetry. There is also a stable linear triplet $^3\Sigma^-$ structure with $C_{\infty h}$ symmetry and a stable quasi-linear singlet $^1A'$ state with C_s symmetry lying 0.2 and 13.8 kcal mol^{-1} above the ground state, respectively. The two triplet structures constitute a quasi-linear−linear Renner−Teller system.[40] The $^3\Sigma^-$ structure has a different electronic configuration than that of either of the triplet states of CCCC and $(CCCB)^-$, with the 8σ orbital being of lower energy than the 1π orbital. (See Figure 2.) According to the AO−MO correlation diagram (Figure 5), the relatively large energy gap (12.4 eV) between the 2s and 2p orbitals of nitrogen indicates much less perturbation to the $2p_z$ orbital from the 2s orbital. This results in virtually no contribution to the 8σ and 9σ molecular orbitals from the 2s atomic orbital, leading to the energy levels of the 8σ and 9σ orbitals lying below $1\pi_y$ and $2\pi_y$. The bond lengths of the $(CCCN)^+$ states show differences compared with those of CCCC and $(CCCB)^-$. Although the CC bonds are essentially double bonds, the CN bond shows significant triple bond character. (See Figure 1 for bond lengths (normal bond lengths: CN double bond 1.30 Å, triple bond 1.16 Å[39]).)

The ground state of $(CCNC)^+$ is the quasi-linear triplet ^3A structure (C_1 symmetry). The bonds of the triplet are mainly double bonds with the terminal NC bond being close to a triple bond, a situation similar to that described above for the two triplet states of $(CCCN)^+$. The singlet state of $(CCNC)^+$ is a bent $^1A'$ structure (C_s geometry) lying 12.0 kcal mol^{-1} above the ground state triplet.

It is of interest to consider the periodic trends in the triplet−singlet energy gaps across the three CCCX systems. As the nuclear charge increases across the period, the valence electrons experience a screened charge, and the incremental change in that charge upon going from anions to cations is unlikely to be significantly different. There will be two opposing effects: (i) because the valence orbitals include *s* character, Coulombic attraction will increasingly favor the singlet upon moving to the right across the period, and (ii) the increased nuclear charge can result in an opposing effect, which arises from the contraction of all MOs in response to the more positive core. The contracted MOs will induce increased Coulomb repulsion between the electrons, which may be relieved by

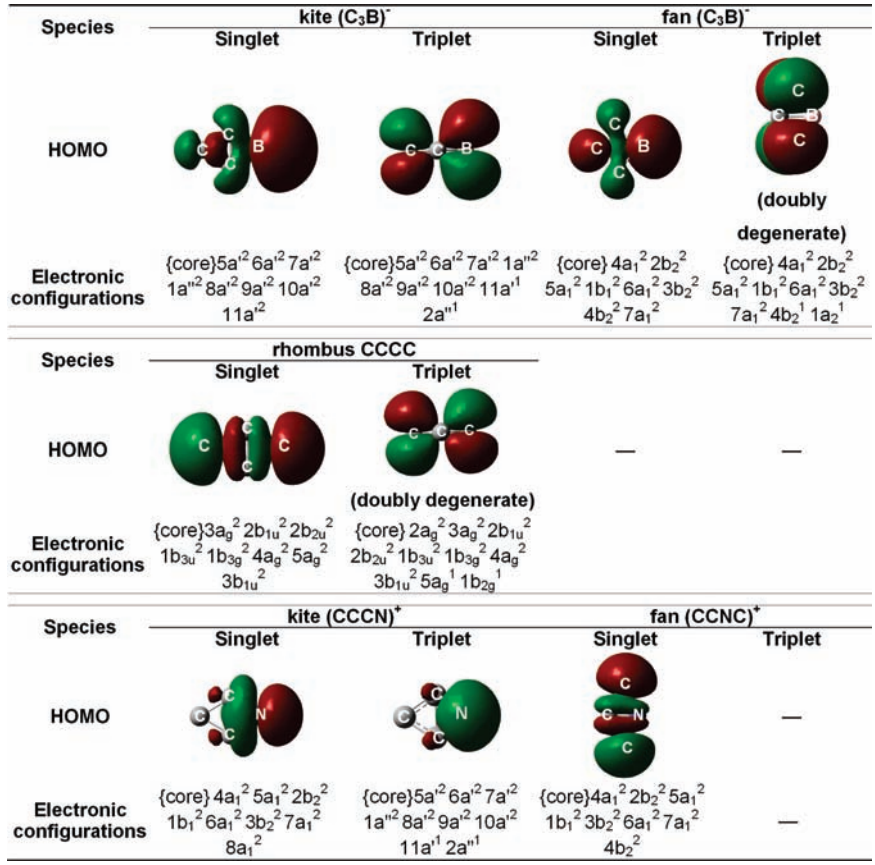

Figure 7. Electronic configurations and 3D HOMOs of the singlet and triplet isoelectronic cyclic structures. B3LYP/6-311+G(3df) level of theory.

promotion of one electron to form the triplet. Furthermore, the favorable exchange energy available to the triplet is similarly affected. In other words, when the interaction is mainly due to Coulomb repulsion of electrons, the exchange energy favors electrons with parallel spins,[42] that is, the triplet states. These opposing effects are important for a comparison of $(CCCB)^-$, CCCC, and $(CCCN)^+$ because the S−T gaps are becoming more positive from $(CCCB)^-$ to $(CCCN)^+$, as shown in Figure 1.

In contrast, there is no *s* character for the HOMOs of singlet $(CCBC)^-$, triplet $(CCBC)^-$, or singlet $(CCNC)^+$. However, there is *s* character for the 13a orbital of triplet $(CCNC)^+$, which is mainly distributed between C_2 and C_3. (The numbered structures are designated in Table 1 of the Supporting Information.) Therefore, the S−T gaps should decrease across the period, as observed, from 16.9 kcal mol^{-1} for $(CCBC)^-$ to 12.0 kcal mol^{-1} for $(CCNC)^+$, leading to the triplet state becoming less favorable.

3.2. Structures of Cyclic Isomers. The geometries and the relative energies of singlet and triplet rhombus C_4 together with kite and fan structures of $(C_3B)^-$ and $(C_3N)^+$ are summarized in Figure 6, whereas full details of these structures are recorded in Table 2 of the Supporting Information. The electronic configuration and HOMO of each of these structures are listed in Figure 7.

Singlet ^1A_g rhombus C_4 of D_{2h} symmetry is the ground state of this system with triplet $^3B_{3u}$ rhombus C_4 (also of C_{2h} symmetry) lying 18.6 kcal mol^{-1} above the ground state. The bonds in the singlet rhombus have more double-bond character than those in the triplet structure. The electronic configuration of the triplet differs considerably from that of the singlet structure (Figure 7), for example. The $5a_g$ orbital is located at a higher energy than $3b_{1u}$. The electronic structure of the singlet shows that $5a_g$ (NHOMO), mainly includes bonding p_y orbitals of C_1 and C_3, and is only 0.001 hartree more stable than $3b_{1u}$ (HOMO) at the B3LYP/6-311+G(3df) level of theory. Therefore, the electrons in either of these two orbitals can be almost equally promoted to the lowest unoccupied molecular orbital (LUMO) ($1b_{2g}$), which consists of empty p_x orbitals perpendicular to the molecular plane. The formation of the triplet increases the bonding density in the p_x orbitals, resulting in an increase in bond lengths. In particular, an electron from $5a_g$ is promoted to $1b_{2g}$, weakening the bond between C_1 and C_3 and increasing the bond length by 0.219 Å.

Like rhombus C_4, the singlet $^1A'$ kite $(C_3B)^-$ of C_s symmetry is the ground state, lying 20.5 kcal mol^{-1} below triplet $^3A''$ rhombus $(C_3B)^-$ (C_s geometry). The bond lengths of the singlet and triplet structures are different. The ground-state singlet CB bonds are single bonds, with the CC bonds showing some double-bond character, whereas all bonds in the triplet have more double-bond character than those of the singlet kite $(C_3B)^-$. For the singlet state, the anionic center is distributed near C_2, which indicates that the HOMO (11a′) involves considerable overlap with the σ bonding orbitals connecting the carbon atoms. When an electron is excited to the LUMO (2a″), which is perpendicular to the HOMO (the molecule plane), the anionic center shifts toward the terminal boron atom. This moves some electron density from C_1−C_2 to the C−N and C_2−C_3 bonds, leading to the outer C−C bonds becoming longer and the C−B and inner C−C bonds getting shorter.

The singlet $^1A_1$ kite $(C_3N)^+$ (C_{2v} symmetry), like its counterparts (above), is also the ground state, only lying 0.2 kcal mol^{-1} below the $^3A''$ triplet of C_s symmetry. The bonding of the $(C_3N)^+$ rhombus structures is different from that of the corresponding $(C_3B)^-$ structures. In the singlet structure, the CC bonds are close to single bonds, whereas the CN bonds are

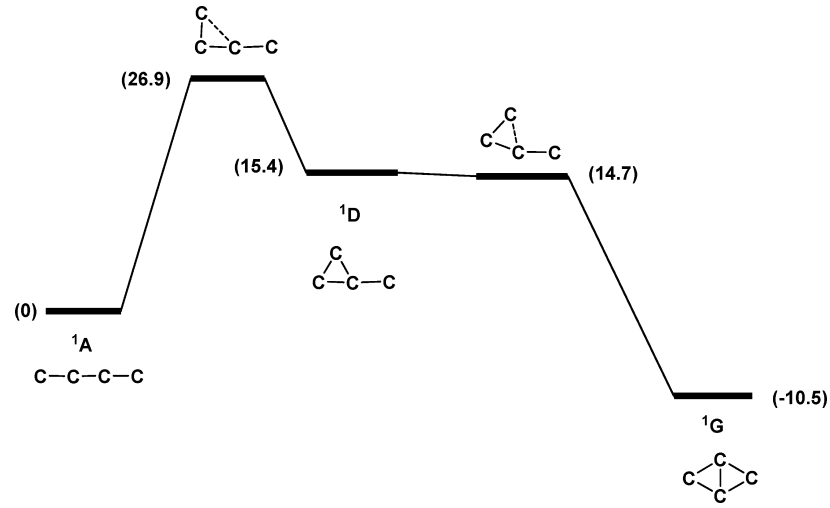

Figure 8. Reaction coordinate profile for the rearrangement of singlet CCCC. CCSD(T)/aug-cc-pVTZ//B3LYP/6-311+G(3df) level of theory. For full details of geometries and energies of minima and transition states, see Table 3 of the Supporting Information.

essentially double bonds. In contrast, for the triplet, the outside CC bonds and the CN bonds have significant double-bond character, whereas the inner CC bond is essentially a single bond. The electronic configuration of the triplet state is exactly the same as that of the triplet kite $(C_3B)^-$, with two unpaired electrons filled in 11a′ and 2a″ respectively. The nonbonding pair of electrons occupies a dominant sp^2-like orbital in the planes (Figure 7), whereas the vertical p_z orbitals are empty. There is considerable overlap with the σ bonding orbitals connecting the C_1, C_3, and N atoms, and the cationic center is approximately located at C_2. The formation of the triplet involves the promotion of one electron from the HOMO (11a′) to the LUMO (2a″), in this case the out of plane p_z orbital; this removes some of the bonding density between the atoms with relative high charge density and meanwhile adds some bonding density between the atoms with low charge density, which makes the C−N bond longer and the C−C bond shorter (Figure 6). The other unpaired electron, located at the 11a′ (NHOMO) orbital, is almost equally distributed between C_1 and C_2, which makes the bond length of C_1-C_2 slightly shorter than that of C_2-C_3.

The fan structures of $(C_3B)^-$ both have C_{2v} symmetry with the ground-state singlet $^1A_1$ lying 11.7 kcal mol^{-1} below triplet $^3A'$. The structures of both states are unusual (Figure 6), with CC bond lengths close to double bonds, whereas the CB bonds show essentially single-bond character. The two electrons of $7a_1$ of the singlet structure are delocalized on C_2, B, and between C_1 and C_3. The triplet structure has two unpaired electrons in doubly degenerated $4b_2$ and $1a_2$ orbitals, which are mainly distributed among C_1C_2B and C_2C_3B, respectively. It is clear that there is no obvious distribution of HOMO electrons between C_2 and B, which may be the reason for the CB single-bond character in both singlet and triplet structures. The shift of the anionic center from kite to fan can explain the change of bond lengths from singlet to triplet. Only the singlet fan state ($^1A'$) of $(C_3N)^+$ is stable. Unlike the fan $(C_3B)^-$ structures, fan $(C_3N)^+$ has bond lengths closer to single than double bonds. The HOMO of fan $(C_3N)^+$ is quite similar to that of rhombus C_4, which indicates more σ delocalization character. The triplet fan $(C_3N)^+$ also has C_{2v} symmetry, yet the HOMO and NHOMO orbitals are nondegenerate, which makes this structure unstable.

The *s* character of the singlet valence orbitals for the kite (rhombus) structures decreases dramatically from a significant value in kite $(C_3B)^-$ to zero in kite $(C_3N)^+$ at the B3LYP/6-311+G(3df) level of theory, which means that the effect of Coulombic attraction is reduced. The effects of contracted MOs repulsion and exchange interaction are more important, and thus the singlet becomes less favorable.

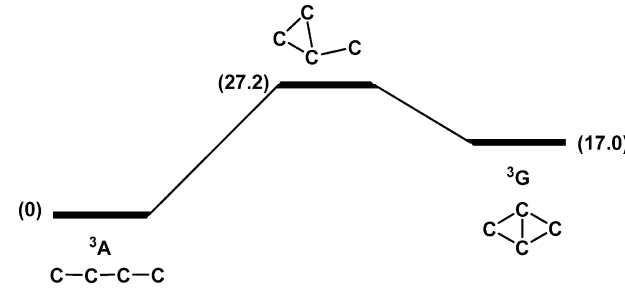

Figure 9. Reaction coordinate profile for the rearrangement of triplet CCCC. CCSD(T)/aug-cc-pVTZ//B3LYP/6-311+G(3df) level of theory. For full details of geometries and energies of minima and transition states, see Table 4 of the Supporting Information.

3.3. Rearrangement Reactions of CCCC, $(CCCB)^-$, and $(CCCN)^+$. The rearrangement/cyclization of CCCC to rhombus C_4 has been described previously, as has the atom scrambling of energized $^{13}CCC^{13}C$ following equilibration with the rhombic isomer.[2] Triplet and singlet reaction coordinate profiles have been recalculated at the CCSD(T)/aug-cc-pVTZ//B3LYP/6-311+G(3df) level of theory to enable direct comparison with the rearrangements of the other systems considered below. Very similar results are obtained here compared with those of the earlier report. The rearrangements of the singlet state and the triplet ground state of CCCC are shown in Figures 8 and 9 respectively, with full details of geometries and energies of minima and transition states recorded in Tables 1 to 4 of the Supporting Information. It can be seen that the rearrangement of singlet linear to rhombic structures involves the C_3-monocyclic intermediate **^{1}D**, which is 15.4 kcal mol^{-1} above **^{1}A**. The energy barrier **TS ^{1}A/^{1}D** for the formation of **^{1}D** from **^{1}A** is 26.9 kcal mol^{-1}. The second cyclization step from **^{1}D** to **^{1}G** is barrierless; that is, **^{1}G** is directly formed once the initial cyclization barrier has been surmounted. The triplet linear structure **^{3}A** may rearrange to triplet rhombic **^{3}G** by overcoming the transition state **TS ^{3}A/^{3}G**, which represents a barrier of 27.2 kcal mol^{-1}. We have investigated the possibility of intersystem crossing between the triplet and singlet forms of CCCC on the singlet and triplet C_4 potential surfaces. The spin orbit coupling constant singlet/triplet CCCC is 19.8 cm^{-1} (at the CASSCF/6-

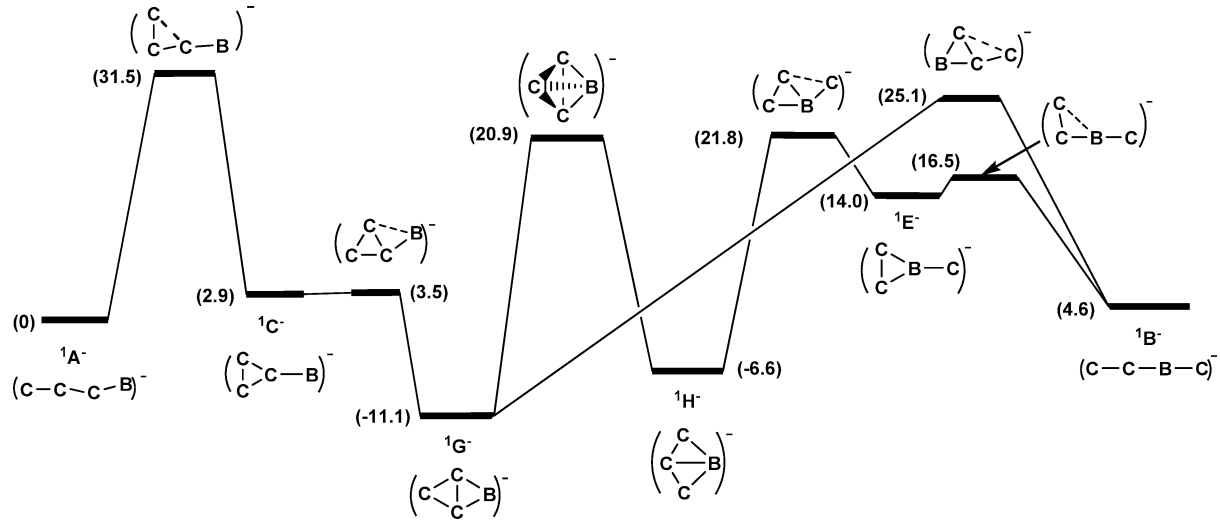

Figure 10. Reaction coordinate profile for the rearrangement of singlet $(CCCB)^-$. CCSD(T)/aug-cc-pVTZ//B3LYP/6-311+G(3df) level of theory. For full details of geometries and energies of minima and transition states, see Tables 5 and 6 of the Supporting Information.

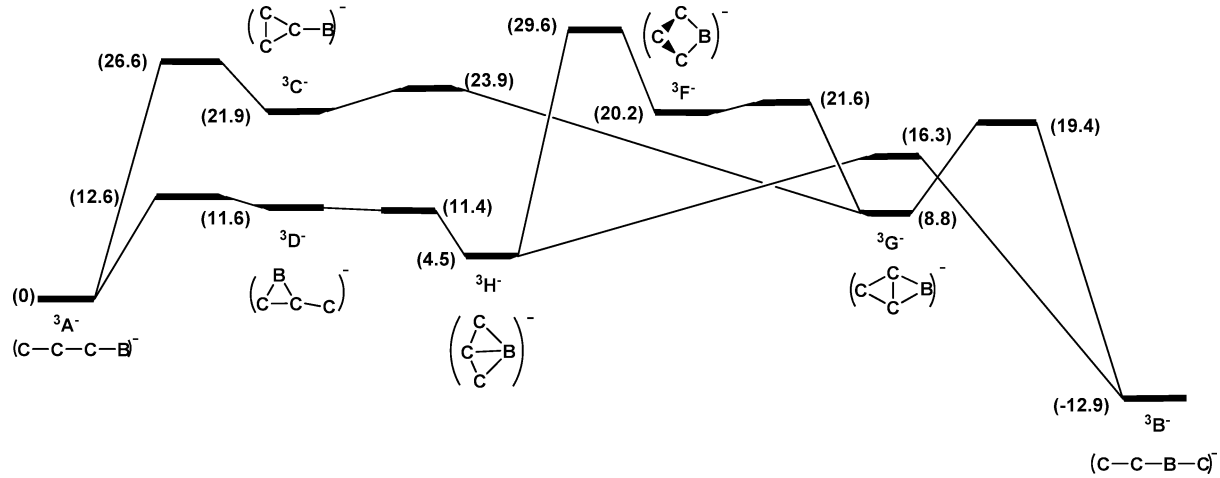

Figure 11. Reaction coordinate profile for the rearrangement of triplet $(CCCB)^-$. CCSD(T)/aug-cc-pVTZ//B3LYP/6-311+G(3df) level of theory. Because of the complexity of this Figure, the transition-state structures have been omitted. For full details of geometries and energies of minima and transition states, see Tables 7 and 8 of the Supporting Information.

311+G(3df) level of theory), this large value indicates that crossing from the bound triplet to the repulsive singlet state should be rapid.[35–38]

The reaction coordinate profiles for the rearrangement of singlet and triplet $(CCCB)^-$ to singlet and triplet $(CCBC)^-$ are shown in Figures 10 and 11, respectively, with full energy and geometric data of minima and transition states listed in Tables 5−8 of the Supporting Information. The rearrangements are more complex than those shown in Figures 8 and 9 (for CCCC) because of the unsymmetrical nature of reactants and products. The processes shown in Figures 10 and 11 are marginally more favorable than those shown in Figures 8 and 9 (for CCCC). Kite and fan structures are interconvertible, but the barriers are significant (^{1}**G** → ^{1}**H** (+33.0 kcal mol^{-1}); ^{3}**G** → ^{3}**H** (+20.8 kcal mol^{-1}) (Figures 10 and 11, respectively)). The energy difference between ground-state singlet $(CCCB)^-$ and the triplet is only 0.6 kcal mol^{-1}, and the spin orbit coupling constant for these two states is 16.7 cm^{-1} (at the CASSCF/6-311+G(3df) level of theory), a value high enough to ensure the likelihood of intersystem crossing between these two potential surfaces at the singlet−triplet minimum energy crossing point.[35–38]

The cation $(CCCN)^+$ has been previously prepared in the mass spectrometer by charge reversal of $(CCCN)^-$.[3] The anion $(CCCN)^-$ is a stable species under the collisional conditions required to convert it to the cation $(CCCN)^+$ (a charge reversal experiment[44,45]). Charge reversal of $(CCCN)^-$, $(^{13}CCCN)^-$, and $(CC^{13}CN)^-$ produces $(CCCN)^+$, $(^{13}CCCN)^+$, and $(CC^{13}CN)^+$, and the decompositions of these cations have been recorded.[3] The spectrum of $(CCCN)^+$ shows peaks due to the losses of C, N, C_2, CN, and C_2N. If there is no scrambling of atoms in the labeled analogues, then $(CC^{13}CN)^+$ should lose only C and CC, whereas $(^{13}CCCN)^+$ should lose ^{13}C and ^{13}CC. Instead, the respective relative abundance ratios for losses of C and ^{13}C are 15:7.7 from $(CC^{13}CN)^+$and 24:14.5 from $(^{13}CCCN)^+$. The corresponding losses of CC and ^{13}CC are 4.8:2.2 from $(CC^{13}CN)^+$ and 1.3:5.2 from $(^{13}CCCN)^+$. These experimental data indicate significant scrambling of carbons in energized $(CCCN)^+$ prior to or during fragmentation.

The reaction coordinate profiles for rearrangement of singlet and triplet $(CCCN)^+$ are shown in Figures 12 and 13, respectively, with full energy and geometric data of minima and transition states listed in Tables 9−12 of the Supporting Information. Consideration of the data shown in Figure 12 shows that one of the processes forming $(CCNC)^+$ (^{1}**B**$^+$) is feasible (overall energy +5.9 kcal mol^{-1}; maximum transition-state barrier 29.4 kcal mol^{-1}). The kite and fan structures are interconvertible (energy difference between ^{1}**G**$^+$ and ^{1}**H**$^+$ is +10.0 kcal mol^{-1}, and the barrier to the higher transition state

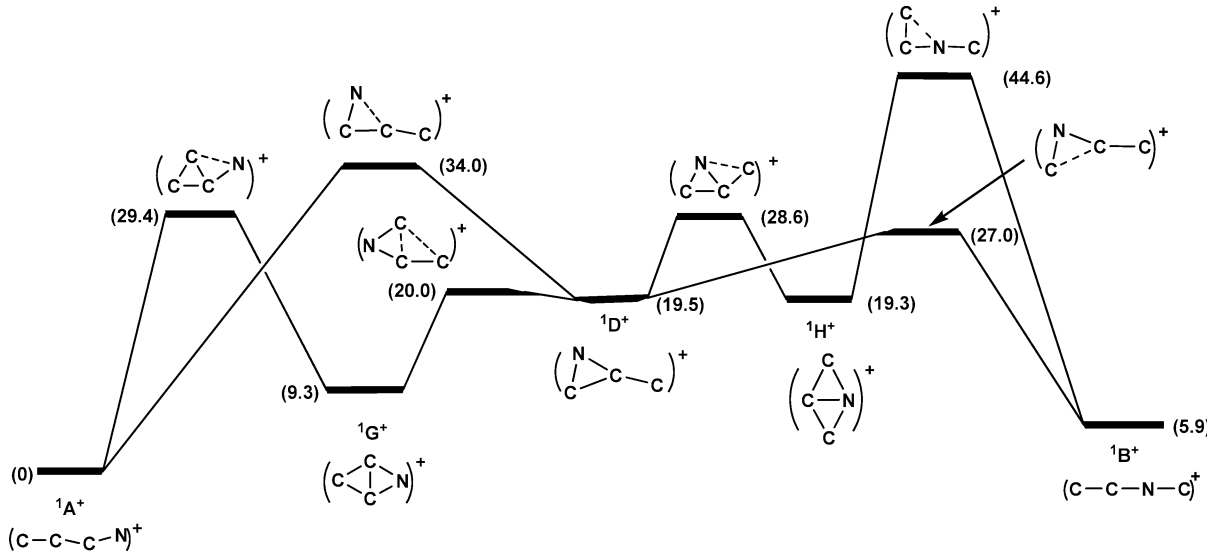

Figure 12. Reaction coordinate profile of the rearrangement of singlet $(CCCN)^+$. CCSD(T)/aug-cc-pVTZ//B3LYP/6-311+G(3df) level of theory. For full details of geometries and energies of minima and transition states, see Tables 9 and 10 of the Supporting Information.

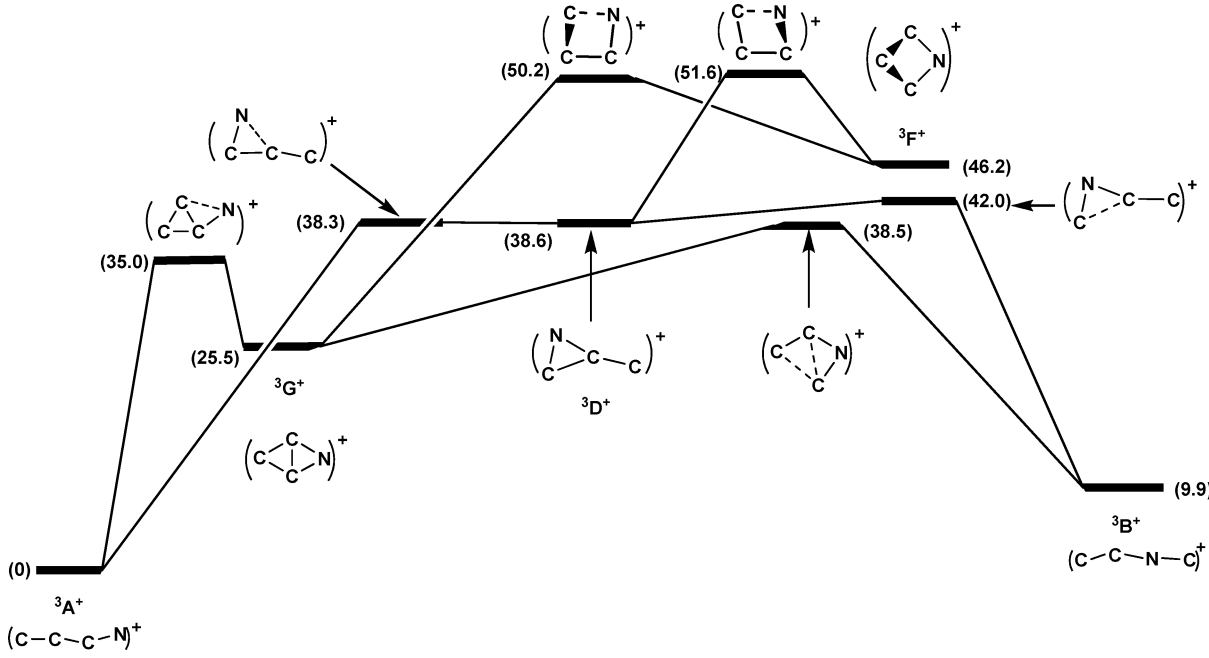

Figure 13. Reaction coordinate profile of the rearrangement of triplet $(CCCN)^+$. CCSD(T)/aug-cc-pVTZ//B3LYP/6-311+G(3df) level of theory. For full details of geometries and energies of minima and transition states, see Tables 11 and 12 of the Supporting Information.

(^{1}**D**$^+$/^{1}**H**$^+$) is 19.3 kcal mol^{-1} (Figure 12)). In contrast, the formation of kite ^{3}**G**$^+$ (+25.0 kcal mol^{-1}) from ^{3}**A**$^+$ with transition-state barrier of 35.0 kcal mol^{-1} is feasible, but further rearrangement to $(CCNC)^+$ (^{3}**B**$^+$) is unfavorable (Figure 13). The fan structure is not stable on this potential surface. The main question is whether ground-state triplet $(CCCN)^+$ can undergo intersystem crossing to singlet $(CCCN)^+$, which can then rearrange to singlet $(CCNC)^+$, as shown in Figure 12. The singlet−triplet gap for $(CCCN)^+$ (^{1}**A**$^+$/^{3}**A**$^+$) is 13.8 kcal mol^{-1}, with a calculated spin−orbit coupling constant of 0 cm^{-1}. The electronic configurations of single and triplet state $(CCCN)^+$ at the crossing point are identical (CASSCF/6-311+G(3df) level of theory), which means that the spin transition will correspond to spin inversion in the same orbital, and such a process is forbidden.[43]

However, the kite structures ^{3}**G**$^+$ and ^{1}**G**$^+$ are minima on their respective potential surfaces, and the energy difference between the two forms is only 0.25 kcal mol^{-1} at the level of theory used in this study. The spin−orbit coupling constant ^{3}**G**$^+$/^{1}**G**$^+$ is 7.1 cm^{-1}. Therefore, it is possible that this triplet/singlet crossing may occur, with the consequence of some conversion to product singlet $(CCNC)^+$.[35–38]

Kite and fan structures of $(C_3B)^-$ and $(C_3N)^+$ are interconvertible by different pathways. A transition state **TS** ^{1}**G**$^-$/^{1}**H**$^-$ is determined for singlet $(C_3B)^-$, whereas the analogous triplet interconversion process involves the fully cyclized tetrahedral structure ^{3}**F**$^-$. In contrast, singlet kite $(C_3N)^+$ first ring opens to form a CCN-monocyclic structure ^{1}**D**$^+$. When energized, the quasi-linear (linear) systems $(CCCB)^-$ and $(CCCN)^+$ may undergo cyclization to planar "rhomboid" or monocyclic systems, which, when ring-opened to form $(CCBC)^-$ and $(CCNC)^+$, may cause scrambling of the carbon atoms of the skeleton. The cyclizations of singlet $(CCCB)^-$ and $(CCCN)^+$ to kite $(C_3B)^-$ and $(C_3N)^+$ are slightly less favorable than

cyclization of singlet linear CCCC to rhombic C_4. Rearrangement of $(CCCN)^+$ to a cyclic system is more facile than cyclization of the corresponding neutral interstellar analogue CCCN, with the initial transition state for the neutral surface being 54.7 kcal mol^{-1} at the CCSD(T)/aug-cc-pVDZ//B3LYP/6-31+G(d) level of theory.[3]

4. Conclusions

The structures of the three isoelectronic molecules, $(C_3B)^-$, C_4, and $(C_3N)^+$, have been investigated theoretically at the B3LYP/6-311+G(3df) level of theory for both singlet and triplet states. There are similarities among the structures and electronic configurations. Linear and planar cyclic structures have been located for all three systems. The singlet−triplet energy gaps for linear and kite structures, calculated at CCSD(T)/aug-cc-pVTZ with zero-point energy corrections, indicate that the effects of Coulombic repulsion are a dominant factor in determining the ground states of these systems. Singlet linear CCCC can form rhombic C_4 via the intermediacy of a C_3-monocyclic minima, whereas triplet CCCC can cyclize directly to the rhombic structure. Rearrangements of linear $(CCCB)^-$ and $(CCCN)^+$ occur via cyclic isomers to form $(CCBC)^-$ and $(CCNC)^+$. Intersystem crossing by spin−orbit coupling (investigated at the CASSCF/6-311+(3df) level of theory) can take place at some stable points, leading to rearrangements occurring via more energetically favorable pathways.

A reviewer has requested that vibrational frequencies for computed minima be included in this article. These data are included in Tables 13−15 of the Supporting Information.

Acknowledgment. We thank the Australian Research Council for funding our cumulene research and for providing a research associate stipend (to T.W.). We thank e-Research (South Australia) for a generous allowance of supercomputer time.

Supporting Information Available: Isoelectronic linear structures, isoelectronic cyclic structures, transition states on potential surface for singlet neutral C_4 and triplet neutral C_4, singlet anion $(C_3B)^-$, triplet anion $(C_3B)^-$, singlet cation $(C_3N)^+$, and triplet cation $(C_3N)^+$ potential surfaces, and vibrational frequencies for computed minima. Valence AO−MO correlation diagrams for CC, linear CC, and CBC. This material is available free of charge via the Internet at http://pubs.acs.org.

References and Notes

(1) Van Orden, A.; Saykally, R. J. *Chem. Rev.* **1998**, *98*, 2313.
(2) Blanksby, S. J.; Schroder, D.; Dua, S.; Bowie, J. H.; Schwarz, H. *J. Am. Chem. Soc.* **2000**, *122*, 7105.
(3) Maclean, M. J.; Fitzgerald, M.; Bowie, J. H. *J. Phys. Chem. A* **2007**, *111*, 12932.
(4) Tran, K. M.; McAnoy, A. M.; Bowie, J. H. *Org. Biomol. Chem.* **2004**, *2*, 999.
(5) Wang, T.; Bowie, J. H. *Phys. Chem. Chem. Phys.* **2009**, *11*, 7553.
(6) Maclean, M. J.; Eichinger, P. C. H.; Wang, T. F.; Fitzgerald, M.; Bowie, J. H. *J. Phys. Chem. A* **2008**, *112*, 12714.
(7) Cernicharo, J.; Goicoechea, J. R.; Benilan, Y. *Astrophys. J.* **2002**, *580*, L157.
(8) Henkel, C.; Jethava, N.; Kraus, A.; Menten, K. M.; Carilli, C. L.; Grasshoff, M.; Lubowich, D.; Reid, A. J. *Astron. Astrophys.* **2005**, *440*, 893.
(9) Brown, R. D.; Godfrey, P. D.; Cragg, D. M.; Rice, E. H. N.; Irvine, W. M.; Friberg, P.; Suzuki, H.; Ohishi, M.; Kaifu, N.; Morimoto, M. *Astrophys. J.* **1985**, *297*, 302.
(10) Hirahara, Y.; Ohshima, Y.; Endo, Y. *Astrophys. J.* **1993**, *408*, L113.
(11) Trimble, V. *Rev. Mod. Phys.* **1975**, *47*, 877.
(12) Apponi, A. J.; McCarthy, M. C.; Gottlieb, C. A.; Thaddeus, P. *Astrophys. J.* **1999**, *516*, L103.
(13) McCarthy, M. C.; Apponi, A. J.; Thaddeus, P. *J. Chem. Phys.* **1999**, *110*, 10645.
(14) Slanina, Z.; Zahradnik, R. *J. Phys. Chem.* **1977**, *81*, 2252.
(15) Martin, J. M. L.; Francois, J. P.; Gijbels, R. *J. Chem. Phys.* **1991**, *94*, 3753.
(16) Martin, J. M. L.; Taylor, P. R. *J. Phys. Chem.* **1996**, *100*, 6047.
(17) Watts, J. D.; Gauss, J.; Stanton, J. F.; Bartlett, R. J. *J. Chem. Phys.* **1992**, *97*, 8372.
(18) Dua, S.; Bowie, J. H. *J. Phys. Chem. A* **2002**, *16*, 287.
(19) Chuchev, K.; BelBruno, J. J. *J. Phys. Chem. A* **2003**, *107*, 1887.
(20) Martin, J. M. L.; Taylor, J. T. *J. Chem. Phys.* **1994**, *100*, 9002.
(21) Leonard, C.; Rosmus, P.; Wyss, M.; Maier, J. P. *Phys. Chem. Chem. Phys.* **1999**, *1*, 1827.
(22) Wyss, M.; Grutter, M.; Maier, J. P. *J. Phys. Chem. A* **1988**, *102*, 9106.
(23) Harland, P. W.; Maclagan, R. *J. Chem. Soc., Faraday Trans.* **1987**, *83*, 2133.
(24) Petrie, S.; McGrath, K. M.; Freeman, C. G.; McEwan, M. J. *J. Am. Chem. Soc.* **1992**, *114*, 9130.
(25) Ding, Y. H.; Huang, X. R.; Li, Z. S.; Liu, J. Y. *THEOCHEM* **1998**, *454*, 61.
(26) Ding, Y. H.; Huang, X. R.; Lu, Z. Y.; Feng, J. N. *Chem. Phys. Lett.* **1998**, *284*, 325.
(27) Parent, D. C. *J. Am. Chem. Soc.* **1990**, *112*, 5966.
(28) Petrie, S.; McGraph, K. M.; Freeman, C. G.; McEwan, M. J. *J. Am. Chem. Soc.* **1992**, *114*, 9130.
(29) Frisch; M. J. Trucks; G. W. Schlegel; H. B. Scuseria; G. E. Robb; M. A. Cheeseman; J. R. Montgomery; J. A., Jr.; Vreven, T.; Kudin; K. N.; Burant, J. C.; Millam, J. M.; Iyengar, S. S.; Tomasi, J.; Barone, V.; Mennucci, B.; Cossi, M.; Scalmani, G.; Rega, N.; Petersson, G. A.; Nakatsuji, H.; Hada, M.; Ehara, M.; Toyota, K.; Fukuda, R.; Hasegawa, J.; Ishida, M.; Nakajima, T.; Honda, Y.; Kitao, O.; Nakai, H.; Klene, M.; Li, X.; Knox, J. E.; Hratchian, H. P.; Cross, J. B.; Bakken, V.; Adamo, C.; Jaramillo, J.; Gomperts, R.; Stratmann, R. E.; Yazyev, O.; Austin, A. J.; Cammi, R.; Pomelli, C.; Ochterski, J. W.; Ayala, P. Y.; Morokuma, K.; Voth, G. A.; Salvador, P.; Dannenberg, J. J.; Zakrzewski, V. G.; Dapprich, S.; Daniels, A. D.; Strain, M. C.; Farkas, O.; Malick, D. K.; Rabuck, A. D.; Raghavachari, K.; Foresman, J. B.; Ortiz, J. V.; Cui, Q.; Baboul, A. G.; Clifford, S.; Cioslowski, J.; Stefanov, B. B.; Liu, G.; Liashenko, A.; Piskorz, P.; Komaromi, I.; Martin, R. L.; Fox, D. J.; Keith, T.; Al-Laham, M. A.; Peng, C. Y.; Nanayakkara, A.; Challacombe, M.; Gill, P. M. W.; Johnson, B.; Chen, W.; Wong, M. W.; Gonzalez, C.; Pople. J. A. *Gaussian 03*; revision C.02 ed.; Gaussian, Inc.: Wallingford, CT, 2004.
(30) Becke, A. D. *Phys. Rev. A* **1988**, *38*, 3098.
(31) Lee, C. T.; Yang, W. T.; Parr, R. G. *Phys. Rev. B* **1988**, *37*, 785.
(32) Dunning, T. H. *J. Chem. Phys.* **1989**, *90*, 1007.
(33) Raghavachari, K.; Trucks, G. W.; Pople, J. A.; Headgordon, M. *Chem. Phys. Lett.* **1989**, *157*, 479.
(34) Woon, D. E.; Dunning, T. H. *J. Chem. Phys.* **1993**, *98*, 1358.
(35) Havlas, Z.; Downing, J. W.; Michl, J. *J. Phys. Chem. A* **1998**, *102*, 5681.
(36) Klessinger, M. *Pure Appl. Chem.* **1997**, *69*, 773.
(37) Michl, J.; Havlas, Z. *Pure Appl. Chem.* **1997**, *69*, 785.
(38) Zimmerman, H. E.; Kutateladze, A. G. *J. Org. Chem.* **1995**, *60*, 6008.
(39) Aylward, G.; Findlay, T. J. V. *SI Chemical Data*, 6th ed.; John Wiley & Sons: New York, 2008.
(40) Renner, R. *Z. Phys.* **1934**, *92*, 172.
(41) Weast, R. C. *Handbook of Chemistry and Physics*; CRC Press: Cleveland, OH, 1975; p 179.
(42) Slater, J. C. *Quantum Theory of Atomic Structure*; McGraw-Hill: New York, 1960; Appendix 19.
(43) Turro, N. J. *Modern Molecular Photochemistry*; University Science Books: Sausalito, CA, 1991; p 202.
(44) Bowie, J. H.; Blumenthal, T. *J. Am. Chem. Soc.* **1975**, *97*, 2959.
(45) Bursey, M. M. *Mass Spectrom. Rev.* **1990**, *9*, 555.

JP907484Z